Complex morphology in a simple chemical system

Ron Devon, Jordan RoseFigura, Daryl Douthat, Jerry Kudenov and Jerzy Maselko*

Received (in Cambridge, UK) 20th December 2004, Accepted 7th February 2005
First published as an Advance Article on the web 17th February 2005
DOI: 10.1039/b419013k

Chemical systems, far from thermodynamic equilibrium, may spontaneously self-construct complex structures mimicking biological structures.

Rotating spirals, fractals, spots and the formation of fingers represent forms that are routinely observed in chemical, physical, geological, cosmological and biological systems.[1] The formation of fingers is probably the most common of shared forms, which have been observed in viscous fingering,[2] in geological systems,[3] propagation of chemical reaction diffusion fronts,[4] chemical reaction diffusion fronts and convection,[5] combustion,[6] frontal polymerization,[7] biological morphogenesis of unicellular algae,[8] chemical precipitation,[9] crystallization,[10] electrodeposition[11] and dissolution.[12] D'Arcy Thompson in his landmark book, "On Growth and Form,"[1] describes many forms common to both the physical and biological worlds. Intriguingly, the mechanisms leading to similar forms are rather different. For example, Nijhout[13] in a chapter, "Patterns and Processes," recently described various mechanisms that result in highly analogous structures. Moreover, it was demonstrated that varied physical and chemical processes could produce highly complex crystallization structures in simple inorganic chemical systems.[15–18] In the present paper, we report the formation of highly complex crystal structures from simple inorganic systems that superficially mimic biological forms. For example, either arboriform (tree like structures) or spongiform crystals will grow out of the solution, depending on the ratio of two ions: $Fe(CN)_6^{3-}$ and Fe^{2+}. Very little is known about such structures.[14]

The two basic morphological forms encountered in this study (Fig. 1 and Fig. 2) are produced by mixing solutions of $K_3Fe(CN)_6$ and $FeSO_4$ in specific proportions; mixtures are left to evaporate in Petri dishes. Arboriform crystals (Fig. 1) are produced when the ratio of $K_3Fe(CN)_6$ to $FeSO_4$ is 4.3:1 to 7.1:1. SEM images of these crystals reveal that individual tree-like branches are internally hollow, much like a capillary tube (Fig. 3). Upward movement of the solution may be driven by capillary action or osmotic pressure. We have not seen any inorganic membranes however we observe abundance of networks of capillary tubs. Therefore we assume that transport is driven exclusively by capillary action.

Together, various interconnecting branches form a continuous internal network or conduit of interconnecting tubules that diverge at different angles. A majority of branches are hexagonal in cross-section, although some also appear pentagonal or rectangular in cross-section.

The fractal dimension was determined using the method described by Du and Stone.[14] The crystals were grown in a Petri dish using solutions of $K_3Fe(CN)_6$ in concentrations of .10M, .20M, .30M, .40M, and .50M. The concentrations of the $FeSO_4$ solution were .07M, .14M, .21M, .28M and .35M (total of 25 solutions). The Petri dishes each were filled with 30 mL of solution and the collection of dishes was then placed in a glass housing to control and slow the rate of evaporation. The fractal dimensions were determined by breaking off branches under magnification, and measuring their length using callipers. Their weight was determined using a scale capable of accuracy to .0001 g. The slope of the line resulting from log-log plots of branch length *vs.* branch

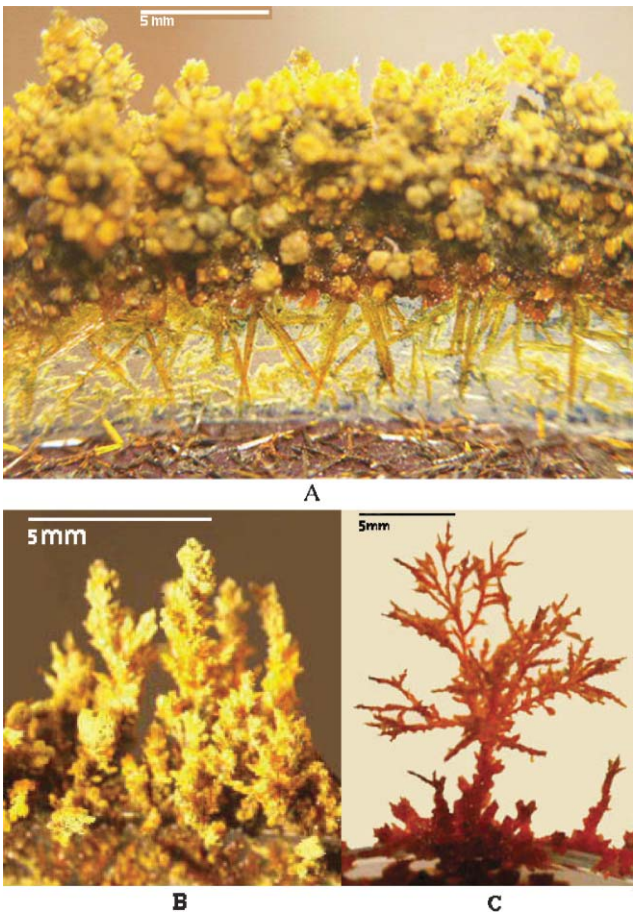

Fig. 1 Chemical trees 1(a). (1.4:1 ratio, Fe^{3+} 0.5M, Fe^{2+} 0.35M, 2.38 fractal dimension). A global view of an inorganic analogue of a mangrove forest that grows in a Petri dish. On the bottom we observe a network of "roots". Attached to the side of the Petri dish, tubular trunks are observed. Above the edge of the dish the "forest canopy" can be seen. 1(b). (3.6:1 ratio, Fe^{3+} 0.5M, Fe^{2+} 0.14M, 1.59 fractal dimension). In this case the trees are developing more defined branches. 1(c). (7.1:1 ratio, Fe^{3+} 0.5M, Fe^{2+}, 0.07M, 1.08 fractal dimension). In this case, the "trees" are sparsely spaced and have only a few thin branches.

*AFJM1@uaa.alaska.edu

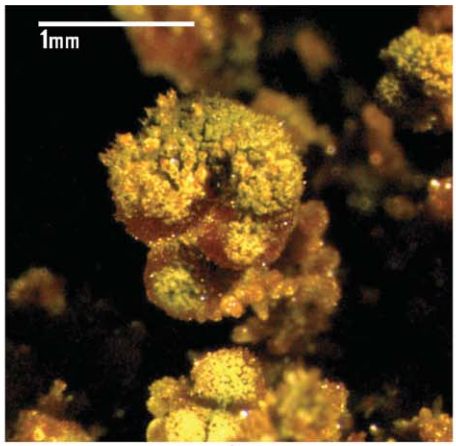

A

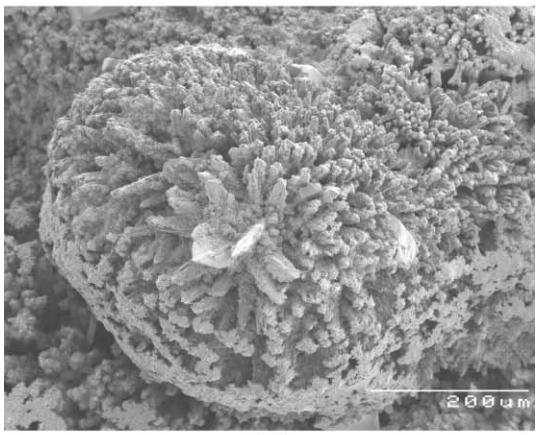

B

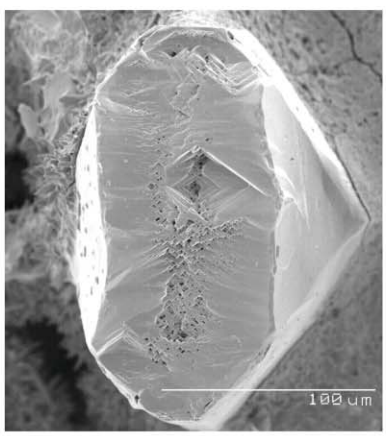

C

Fig. 2 Chemical sponges. (1.8:1 ratio, Fe^{3+} 0.5M, Fe^{2+} 0.28, 2.14 fractal dimension). The fractal structure is visible in 2(a) where succeeding semi-spheres are visible. 2(b). Electron microscope imagery of the smallest semi-sphere. 2(c). Upon fracture of the sponge, one observes a cross sectional view which displays the channels used in transporting the building material.

weight gives the fractal dimension of the structure (Fig. 4A). The dimension of a perfect crystal is 3.0 and for a tube without branches is equal to 1.0. In effect, the shape of the arboriform crystal varies with the ratio of $K_3Fe(CN)_6$ to $FeSO_4$: trees become less dense. The fractal dimension is a function of the $K_3Fe(CN)_6$: $FeSO_4$ ratio (Fig. 4B) and decreases asymptotically to 1.0 as the ratio increases.

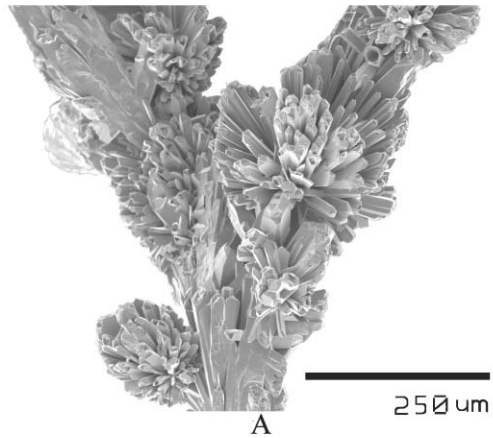

A

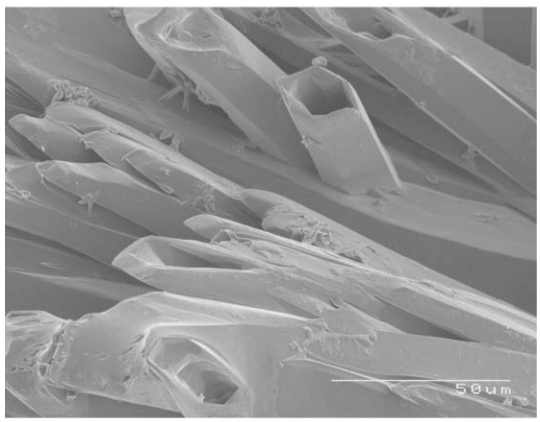

B

Fig. 3 Detailed structure of tree branches. (7.1:1 ratio, Fe^{3+} 0.5M, Fe^{2+} 0.07M, 1.08 fractal dimension). 3(a). Magnification of the bifurcation of 2(b). 3(b). Magnification of the tree branches in 3(a), showing in detail the branched structure and hollow interior of tubes used in transporting the material for growth.

Spongiform crystal structures (Fig. 2) that appear exceedingly more porous and bulkier than the arboriform structures are typically produced when the $K_3Fe(CN)_6$ to $FeSO_4$ ratio ranges from 1.4:1 to 4.3:1. These crystals would sometimes grow together in clusters, always lacked branches, and instead were composed of numerous semi spheres.

Every semi sphere is constructed from numerous smaller semi spheres (Fig. 2A, B), which is consistent for fractal structures. The spongiform crystal is highly porous, which facilitates internal transport of $K_3Fe(CN)_6$–$FeSO_4$ mixtures. SEM imagery of fractured spongiform crystals (Fig. 2C) suggests that the growth mechanism is different compared to that of arboriform crystals. For example, the numerous internal capillary tubules exhibit a four-sided rhomboidal symmetry, and are surrounded by a dense crystal matrix. The honeycomb appearance of the capillary tubules suggests that capillary action is largely responsible for material transport to the surface. Moreover, there are no transitional forms intermediate between spongiform and arboriform crystals; in some cases both forms are represented in a single solution.

We hypothesize that arboriform crystal formation occurs in several steps. An intricate network of porous tubular "roots" develops on the bottom and then grows up the sides of a Petri dish as fluid levels evaporate (Fig. 1). They appear similar in form to

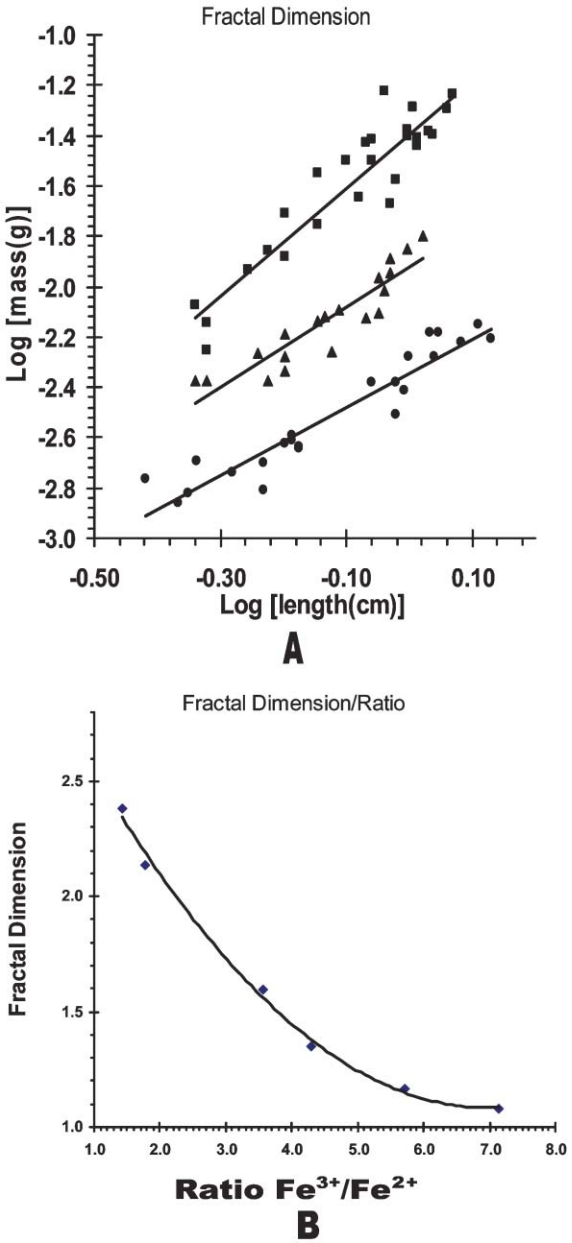

Fig. 4 , Mass of a branch of a salt tree as a function of length for ratios of Fe^{3+}/Fe^{2+} are plotted in A. (Squares are 1.8:1 with fractal dimension of 2.14, triangles are 3.6:1 with fractal dimension of 1.59, diamonds are 5.0:1 with fractal dimension of 1.35.) The slopes represent the fractal dimensions of the crystals and are plotted as a function of ratio in B.

the prop or stilt roots of red mangrove trees.[19] These roots converge and fuse to form the basal trunks of crystal trees, forming a complex conduit through which fluids are transported to the growing branches.

Tree growth ceases if the "prop root" system is severed. Branching commences once the trunk grows above the edge of the dish. We hypothesize that branches grow as solution is transported through internal capillaries to the surface where it both vaporizes and crystallizes around distal tubule openings. For example, solution was actually observed on the surface of spongiform crystals. We find the form displayed by "root" systems of these inorganic tree-like crystals and the prop or stilt roots of red mangrove trees interesting. The root systems of arboriform crystals and mangroves grow in opposite directions. The roots of both systems function to transport fluids to the growing branches and, in the case of mangroves, leaves. Unlike mangroves, it appears that capillaries of arboriform crystals do not transport fluids against diffusion gradients to the roots.

The mechanism of crystalline sponge formation is probably different, and surmises the existence of complex interconnecting networks of capillary tubes analogous to those described in leuconoid poriferan sponges.[20] The presence of such complex networks may be partly dependent on the ratio of solutions used and to their ionic interactions. In leuconoid sponge's incurrent channels that transport water, oxygen and food particles repeatedly branch into smaller tubules that eventually open into chambers lined with flagellated collar cells where fluids containing food and gases are processed. Although the analogy between leuconoid and crystalline sponges is tenuous, fluid transport and crystal growth in inorganic sponges must reflect a quantitative relationship involving the vaporization, osmotic migration of salts through a highly porous network of minute channels and precipitation. The mechanism describing this association is under investigation.

Ron Devon, Jordan RoseFigura, Daryl Douthat, Jerry Kudenov and Jerzy Maselko*
Department of Chemistry, Department of Biological Sciences, Department of Physics and Astronomy, University of Alaska, Anchorage. E-mail: AFJM1@uaa.alaska.edu; Fax: (907) 786 4607; Tel: (907) 786 4697

Notes and references

1 D. W. Thompson, *On Growth and Form*, Cambridge at the University Press, Cambridge, UK, 1942.
2 V. Horvath, T. Vicsek and J. Kertesz, *Phys. Rev. A.*, 1987, **35**, 2353–2356.
3 P. Ortoleva, J. Chadam, E. Merino and A. Sen, *Am. J. Sci.*, 1987, **287**, 1008–1040.
4 St. Scott and K. Showalter, *J. Phys. Chem.*, 1992, **96**, 8702–8711.
5 J. Pojman, A. Komlosi and I. Nagy, *J. Phys. Chem.*, 1996, **100**, 16209–16212.
6 G. Lubkin, *Phys. Today*, 1999, January, 19–19.
7 J. Pojman, R. Craven, A. Khan and W. West, *J. Phys. Chem.*, 1992, **96**, 7466–7472.
8 P. Pelce and A. Pocheau, *J. Theor. Biol.*, 1992, **156**, 197–214.
9 J. Maselko, A. Geldenhuys, J. Miller and D. Atwood, *Chem. Phys. Lett.*, 2003, **373**, 563–567.
10 P. Radnoczy, T. Vicsek, L. Sander and D. Grier, *Phys. Rev. A*, 1987, **35**, 4012–4015.
11 M. Matsushiba, M. Sano, Y. Hayakawa, H. Honjo and Y. Sawada, *Phys. Rev. Lett*, 1984, **53**, 286–289.
12 G. Daccord and R. Lenormand, *Nature*, 1987, **325**, 41–43.
13 H. Nijhout, L. Nadel and D. Stein, Editors, *Pattern Formation in Physical and Biological Sciences*, Westview Press, Boulder, CO, 1997.
14 R. Du and H. Stone, *Phys. Rev. E*, 1996, **53**, 1994–1997.
15 A. Heuler, D. Finhk, V. Laraia, J. Arias, P. Calvert, K. Kendall, G. Messing, J. Blackwell, P. Rieke, D. Thomson, A. Wheeler, A. Veis and A. Caplan, *Science*, 1992, **255**, 1098–1105.
16 H. Yang, A. Kuperman, N. Coombs, S. Mamiche-Afra and G. Ozin, *Nature*, 1996, **379**, 703–705.
17 P. Bianconi, J. Li and A. Strzelecki, *Nature*, 1991, **349**, 315–317.
18 D. C. Ford and P.W. Williams, *Karst Geomorphology and Hydrology*, Unvin Hyman, 1989.
19 P. J. Hogarth, *The Biology of Mangroves (Biology of Habitats)*, Oxford University Press, Oxford, UK, 2000.
20 R. C. Brusca and G. J. Brusca, *Invertebrates*, Sinauer & Associates, Sunderland, MA, 2002.

